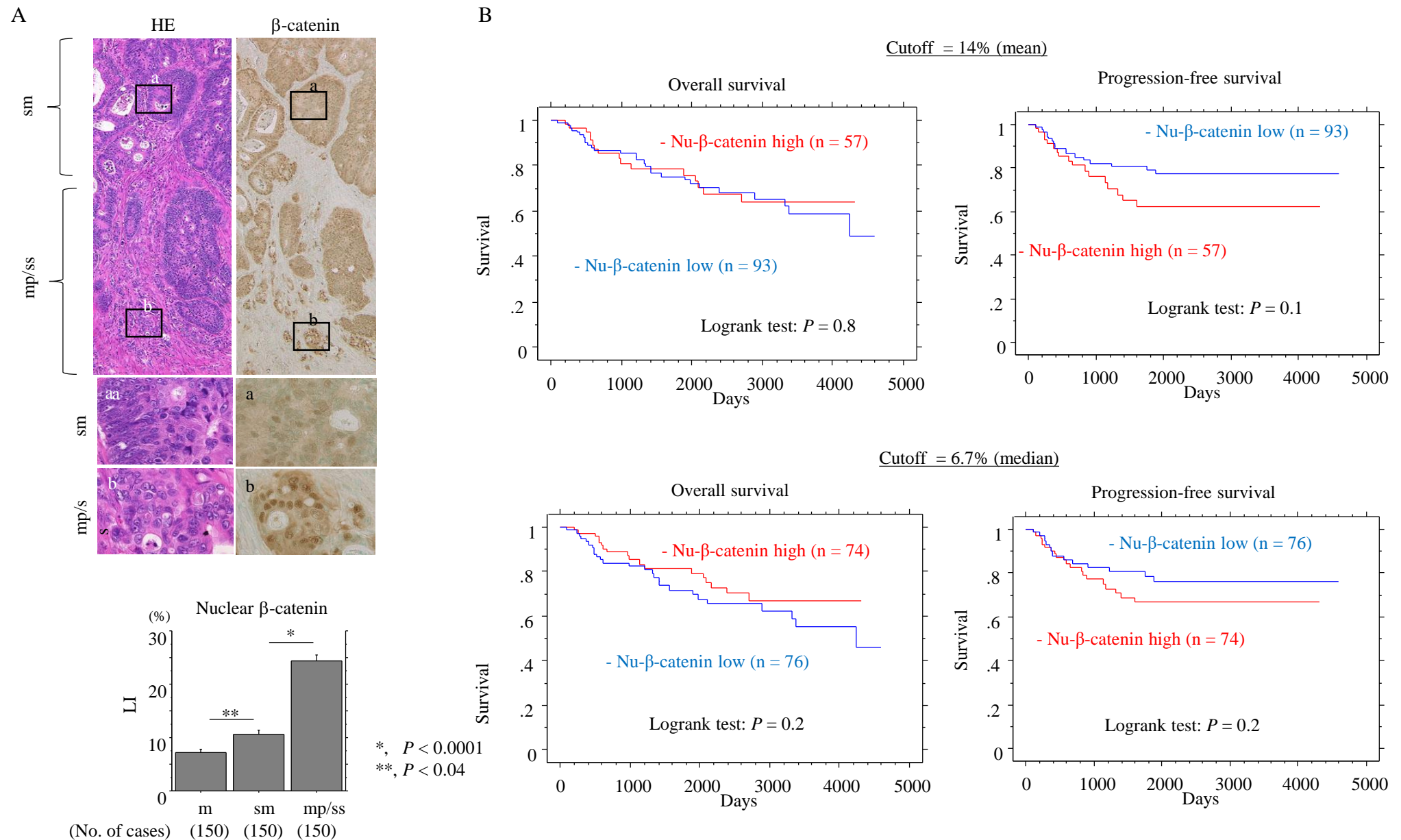
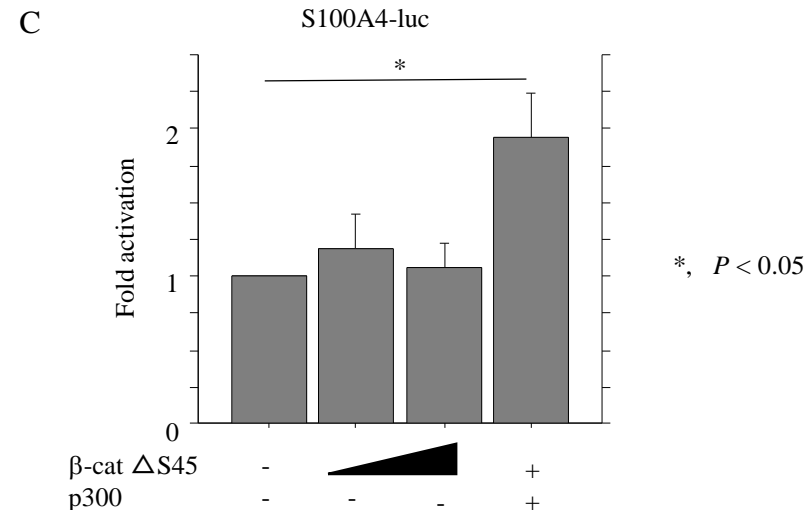
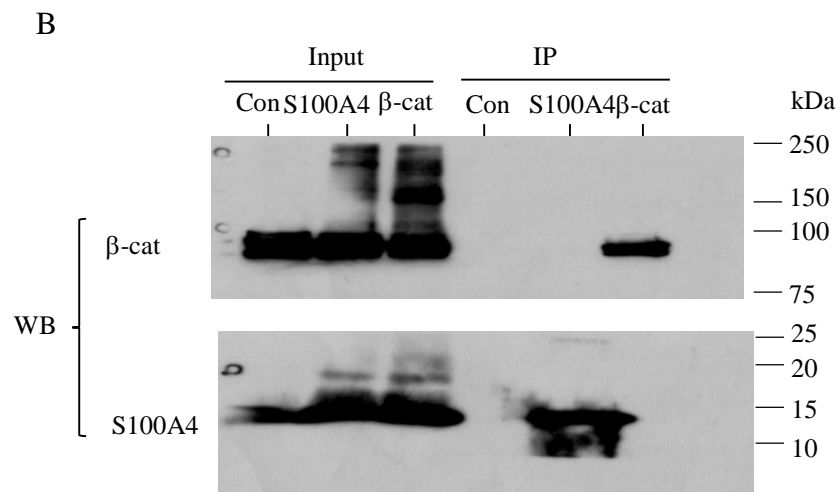
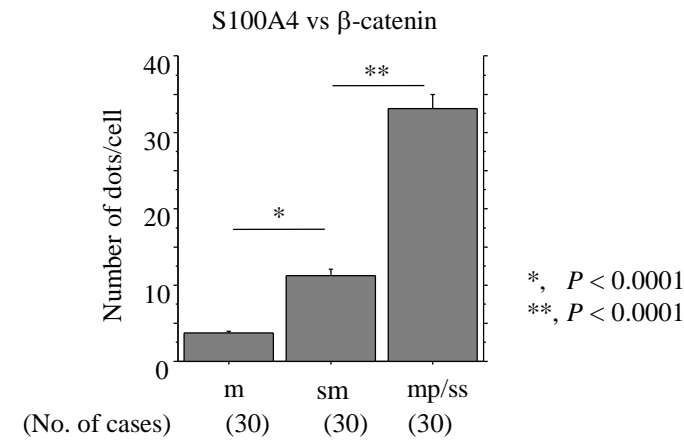
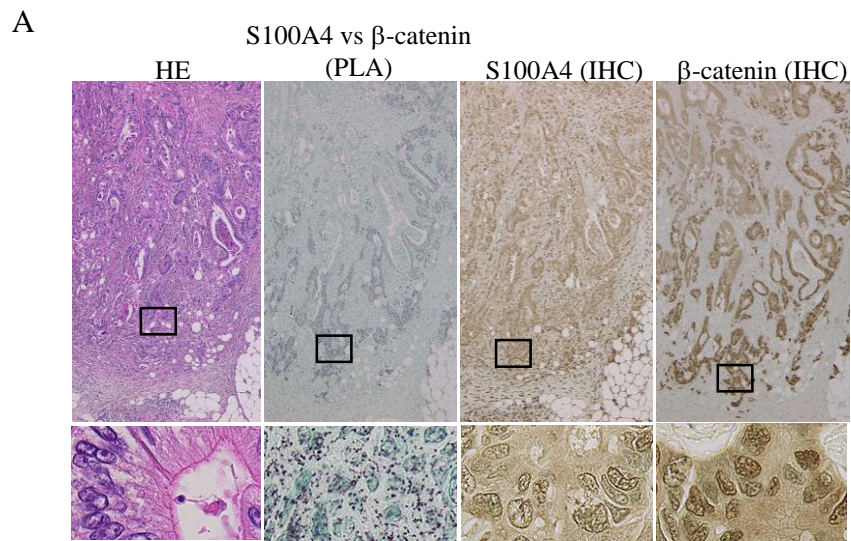


**Supplementary Figure S1.** (A,B) Dot plot analyses for S100A4 scores (A) and nuclear  $\beta$ -catenin LIs (B) in 150 Ad-CRC cases (left) and 150 NCRT-treated LAd-RC cases (right). The data are shown as mean  $\pm$  SD. Based on the mean - standard deviation (SD), mean, or median values as cutoffs, cases are divided into two (high versus low expression) categories.

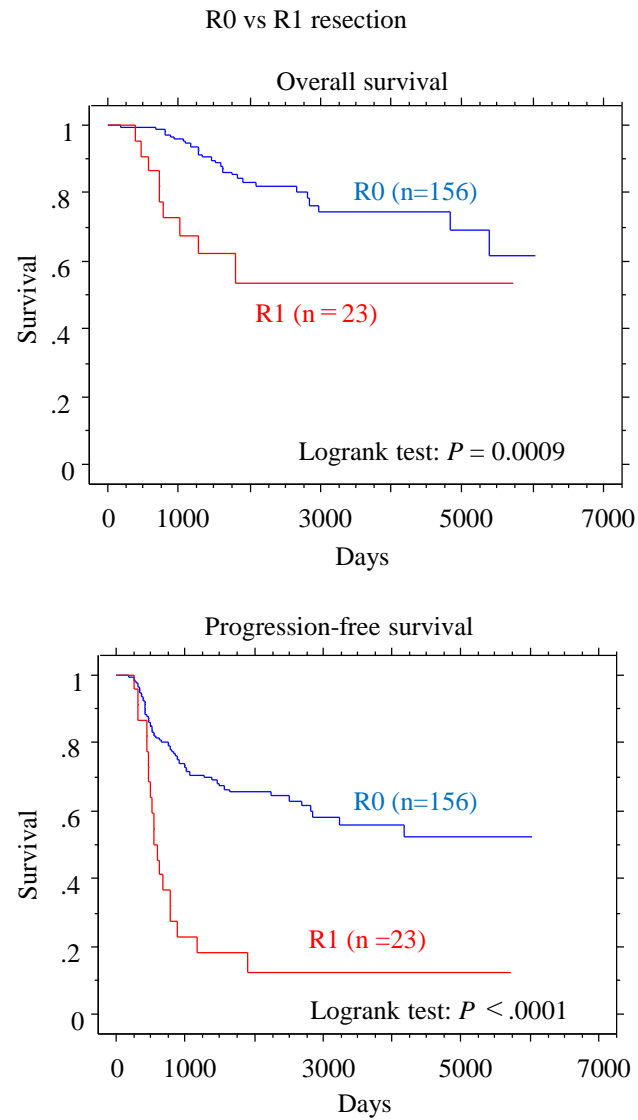


**Supplementary Figure 2. Nuclear  $\beta$ -catenin accumulation in Ad-CRC.** (A) Upper: staining with HE and IHC for  $\beta$ -catenin in Ad-CRC. Note the high levels of nuclear  $\beta$ -catenin at the invasive front in Ad-CRC. The closed boxes in the lower panels are magnified in the insets. Original magnification, x40 and x400 (insets). Lower: nuclear  $\beta$ -catenin LIs between mucosal (m), submucosal (sm), and muscularis propria (mp)/subserosal (ss) lesions of Ad-CRC. The data are presented shown as mean  $\pm$  SD. Statistical analyses were carried out using the Mann-Whitney U-test. (B) OS (left) and PFS (right) relative to nuclear  $\beta$ -catenin LI values (low versus high accumulation) based on the mean (upper) and median values (lower) as cutoffs in Ad-CRC. n, number of cases.

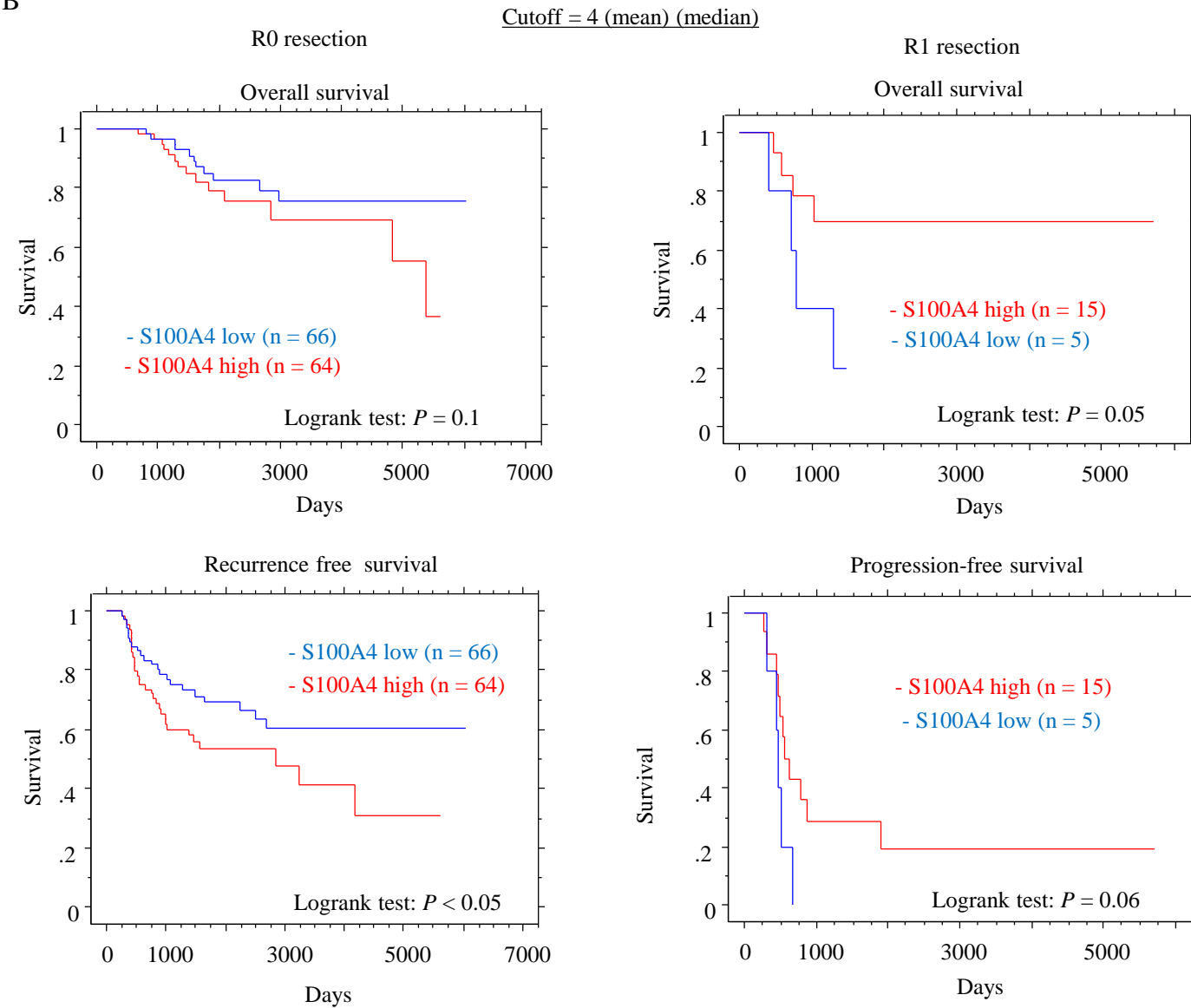


**Supplementary Figure S3. Interaction between S100A4 and  $\beta$ -catenin in CRC cells.** (A) Left: PLA assay for the S100A4/ $\beta$ -catenin interaction, as well as IHC for S100A4 and  $\beta$ -catenin, in Ad-CRC. Note the small aggregated dots in nuclear/cytoplasmic compartments of the tumor cells. The closed box in the PLA panel is magnified in the inset. Original magnification, x100 and x400 (inset). Right: numbers of PLA scores for S100A4/ $\beta$ -catenin combination between mucosal (m), submucosal (sm), and muscularis propria (mp)/subserosal (ss) lesions of Ad-CRC. The data are shown as mean  $\pm$  SD. Statistical analyses were carried out using the Mann-Whitney U-test. (B) After immunoprecipitation (IP) with the indicated antibodies using HCT116 cell lysates, western blot assay (WB) with anti- $\beta$ -catenin (upper panel) and anti-S100A4 antibodies (lower panel) was carried out. Input was 5% of the total cell extract. Normal rabbit IgG was used as a negative control. The reconstructed images of all blots with membrane edges visible are shown because some of the original full-length blots were cut prior to hybridization with antibodies. The experiments were performed in triplicate. (C) HCT116 cells were transfected with S100A4 promoter luciferase (luc), together with  $\beta$ -catenin  $\Delta$ S45 and p300, using LipofectAMINE PLUS. Relative activity was determined based on arbitrary light units of luciferase activity normalized to pRL-TK activity. The activities of the reporter plus the effector relative to that of the reporter plus empty vector are shown as means  $\pm$  SDs. The experiments were performed in triplicate.

A



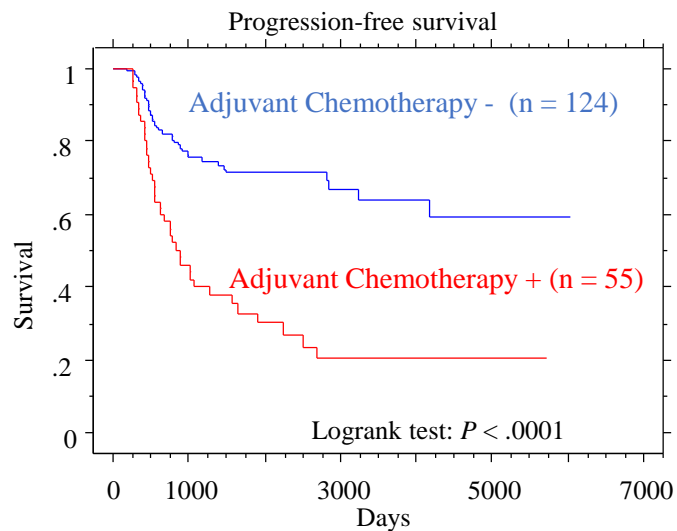
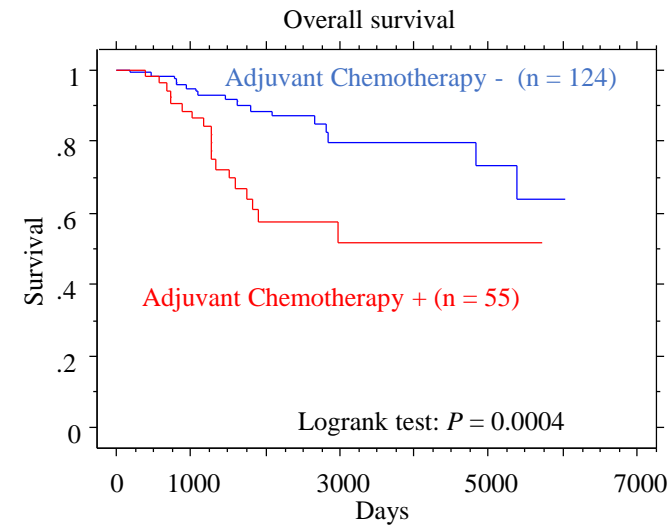
B



**Supplementary Figure S4. Prognostic significance of residual (R) tumor status in NCRT-treated LAd-RC.** (A) OS (upper) and PFS (lower) relative to residual tumors (R0 versus R1 resection) in NCRT-treated RC. (B) OS (upper) and RFS (lower-left) or PFS (lower-right) relative to S100A4 scores (low versus high expression) based on the mean and median values as cutoff in NCRT-treated RC with R0 (left) and R1 resection (right). n, number of cases.

A

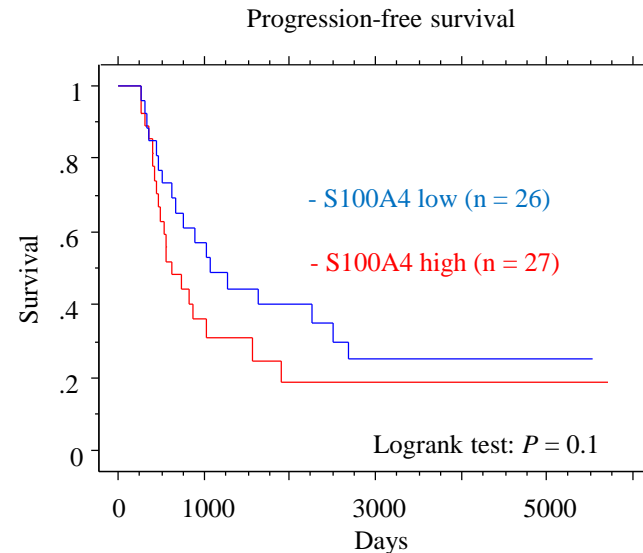
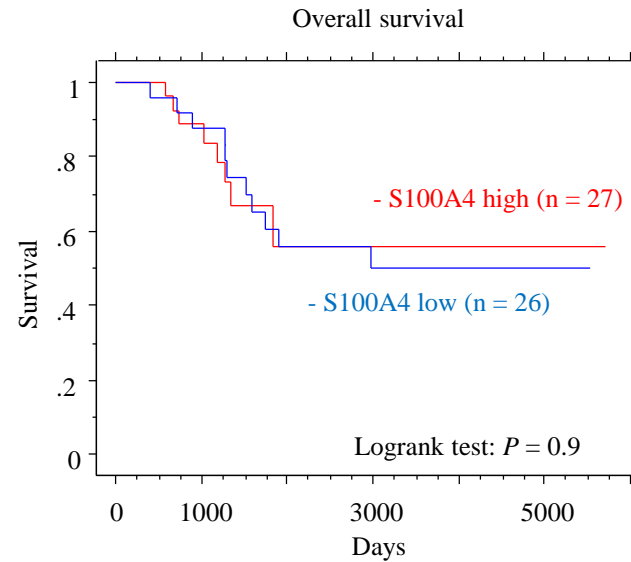
## Post-surgical adjuvant chemotherapy



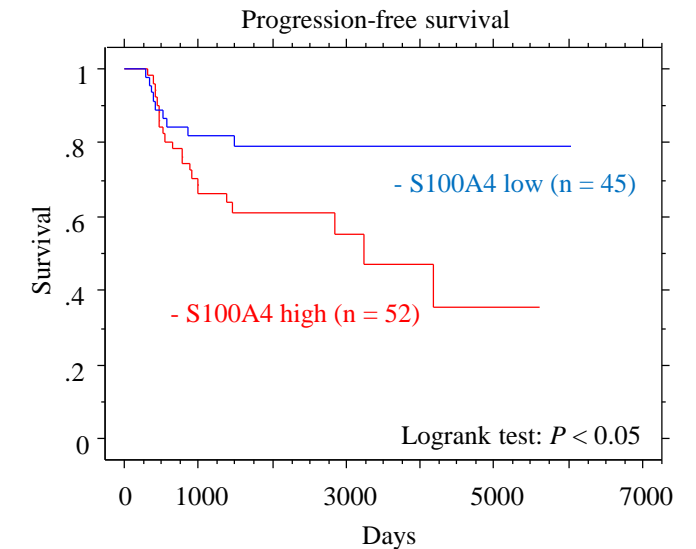
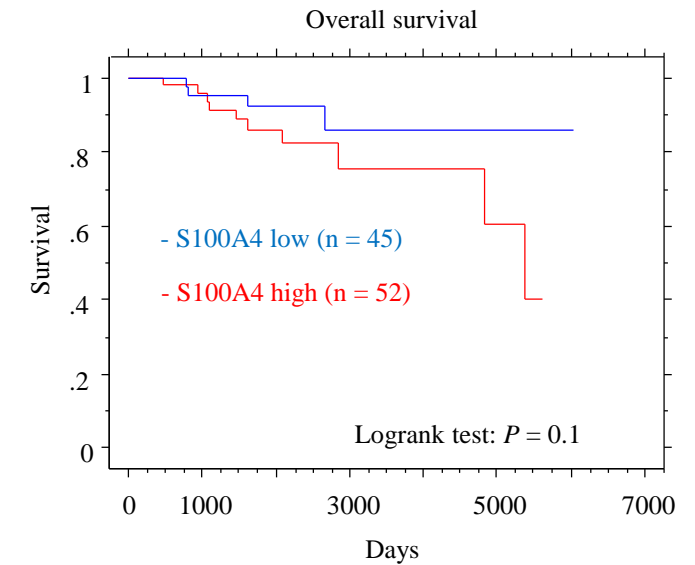
B

Cutoff = 4 (mean) (median)

## S100A4 status with adjuvant chemotherapy

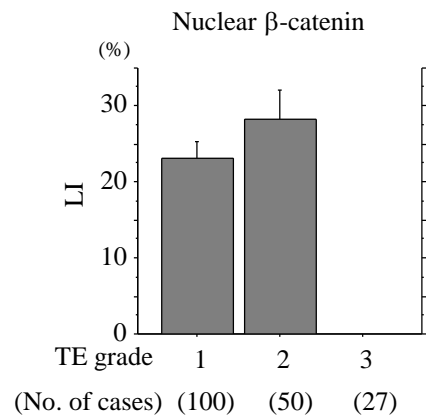
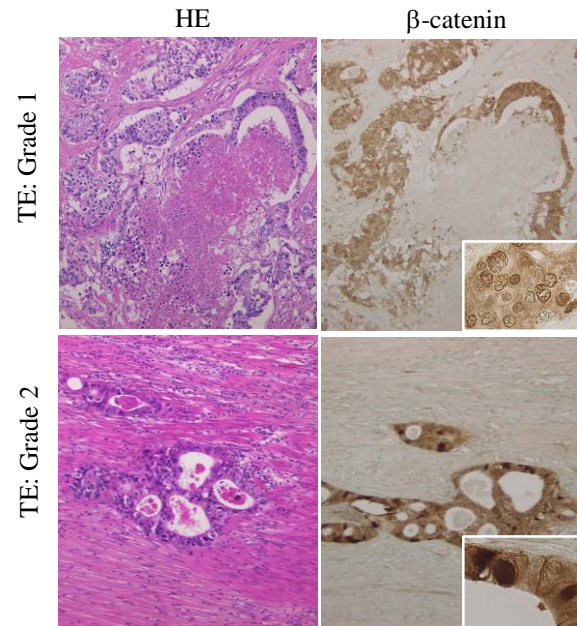


## S100A4 status without adjuvant chemotherapy

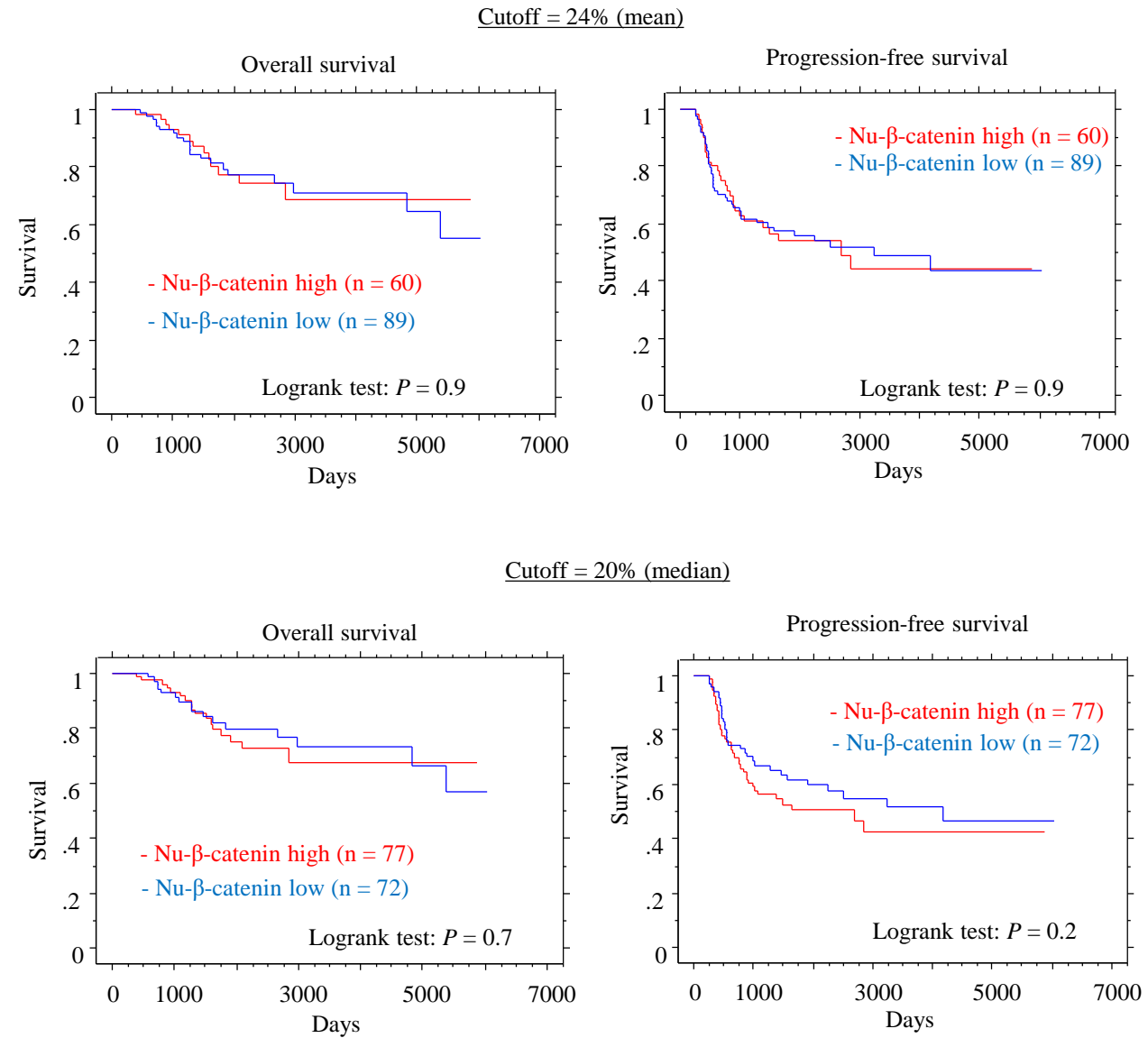


**Supplementary Figure S5. Prognostic significance of post-surgical adjuvant chemotherapy in NCRT-treated LAd-RC.** (A) OS (upper) and PFS (lower) relative to post-surgical adjuvant chemotherapy [Yes (+) versus No (-)] in NCRT-treated RC. (B) OS (upper) and PFS (lower) relative to S100A4 scores (low versus high expression) based on the mean and median values as cutoff in NCRT-treated RC with (left) and without post-surgical adjuvant chemotherapy (right). n, number of cases.

A

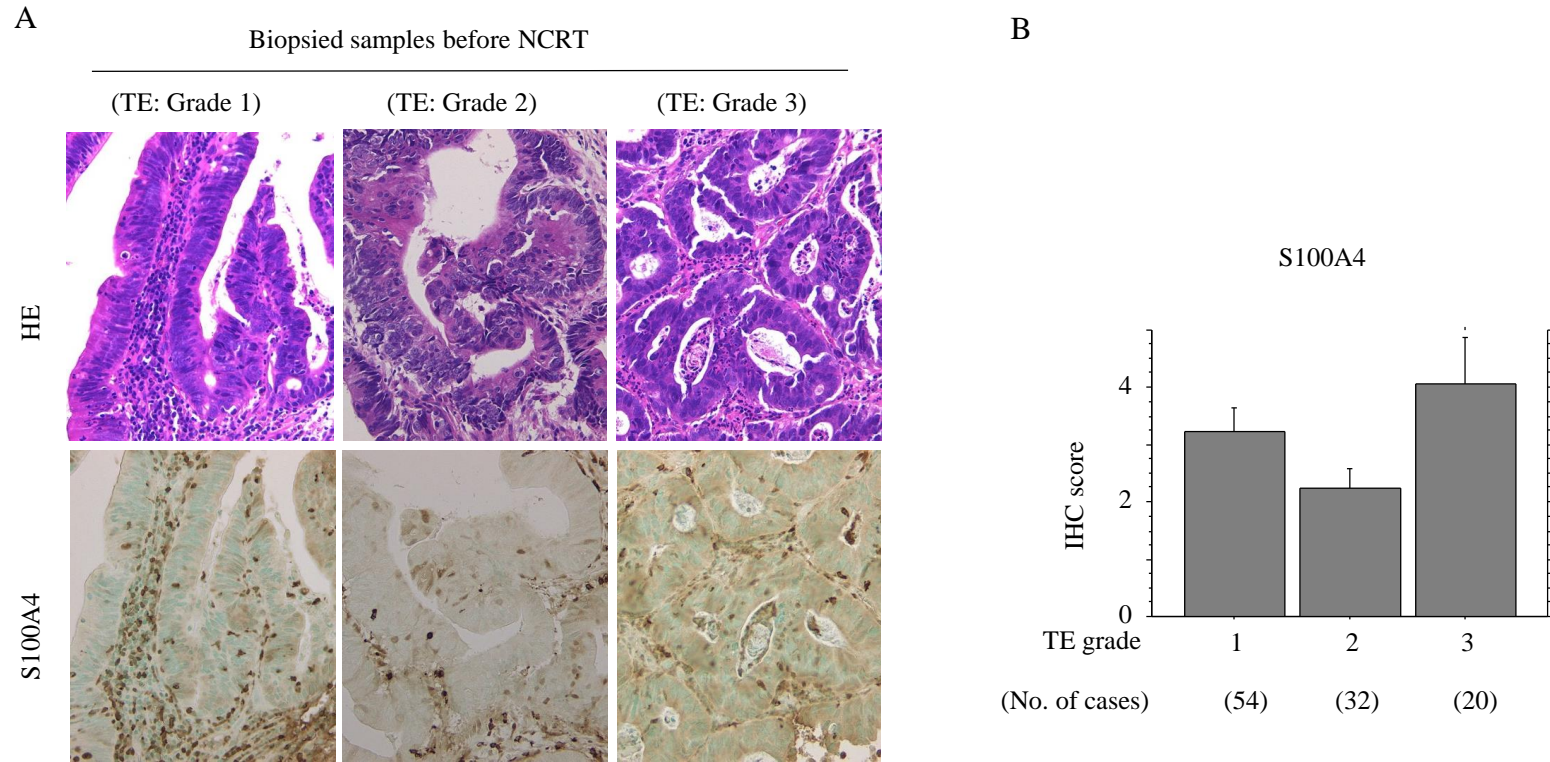


B

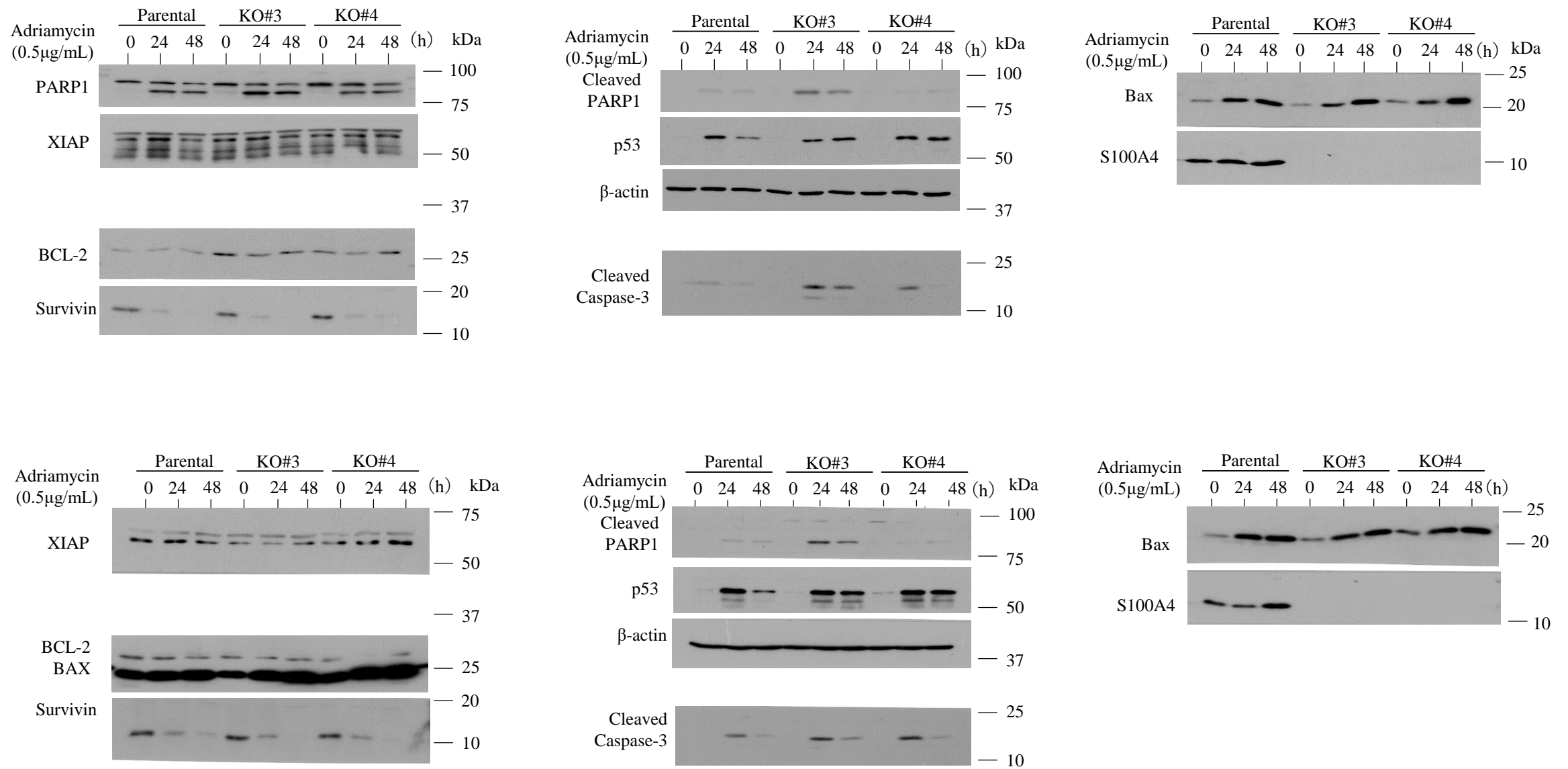


**Supplementary Figure S6. Relationship between nuclear  $\beta$ -catenin accumulation and NCRT resistance in LAd-RC.** (A) Upper: staining with HE and IHC for  $\beta$ -catenin in samples of LAd-RC cases that respond poorly to NCRT (TE: Grade 1) or respond moderately (TE: Grade 2). The closed boxes in the IHC panels are magnified in the insets. Original magnification,  $\times 100$  and  $\times 400$  (insets). Lower: nuclear  $\beta$ -catenin LIs in samples from NCRT-treated LAd-RC patients. The LIs are shown as mean  $\pm$  SD. (B) OS (left) and PFS (right) relative to nuclear  $\beta$ -catenin (low versus high LIs) based on the mean (upper) and median LI values (lower) as cutoffs in LAd-RC receiving NCRT. N, number of cases.



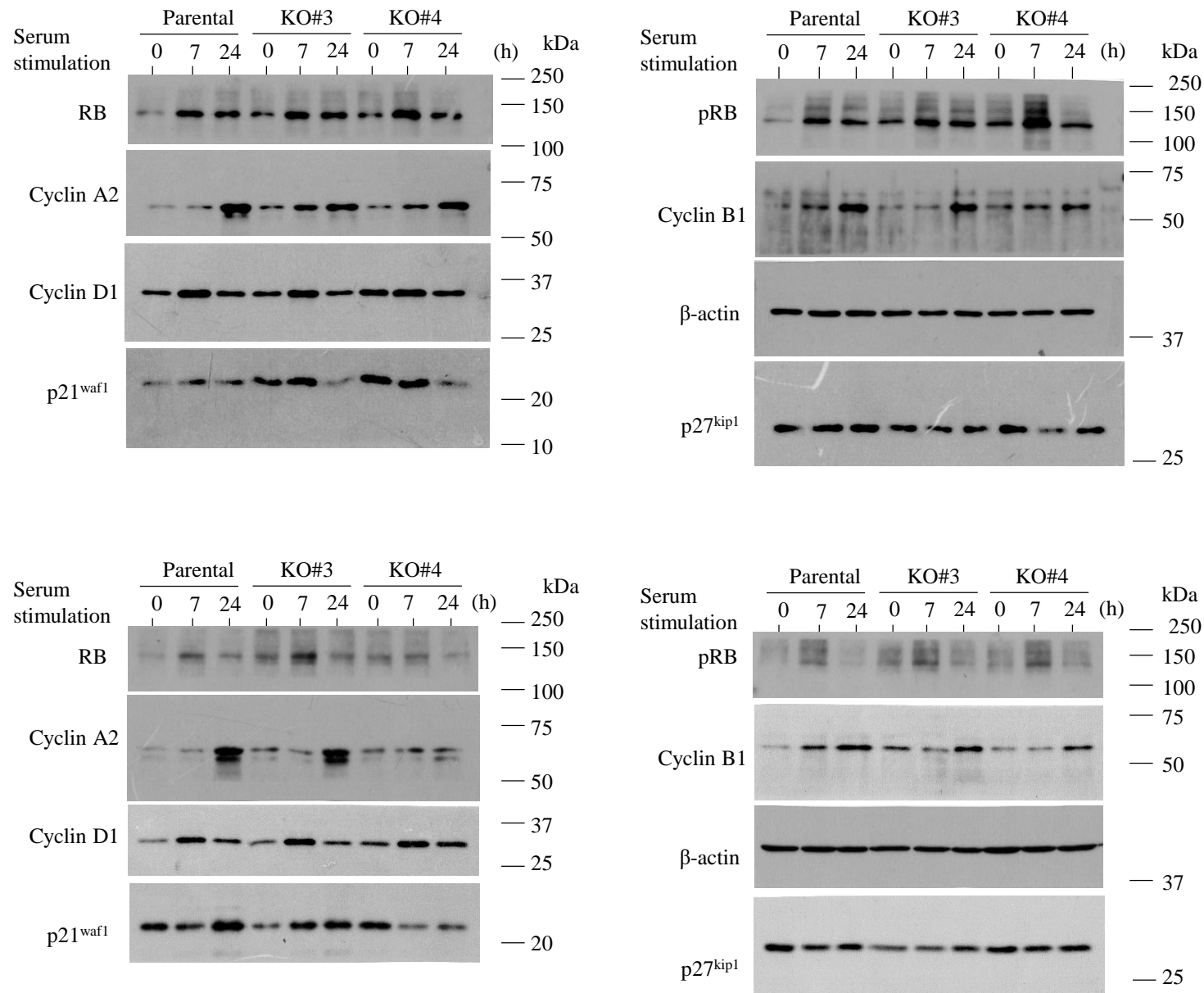


**Supplementary Figure S7. Relationship between S100A4 expression in pretreatment-biopsied samples and TE grade in surgical specimens of NCRT-treated LAd-RC.** (A) Staining with HE and IHC for S100A4 in pretreatment LAd-RC patient biopsies from TE: Grade 1 (left), TE: Grade 2 (middle), and TE: Grade 3 (right). Original magnification, x200. (B) IHC scores for S100A4 in pretreatment biopsied samples from TE grade 1, 2, and 3. The scores are shown as mean  $\pm$  SD.

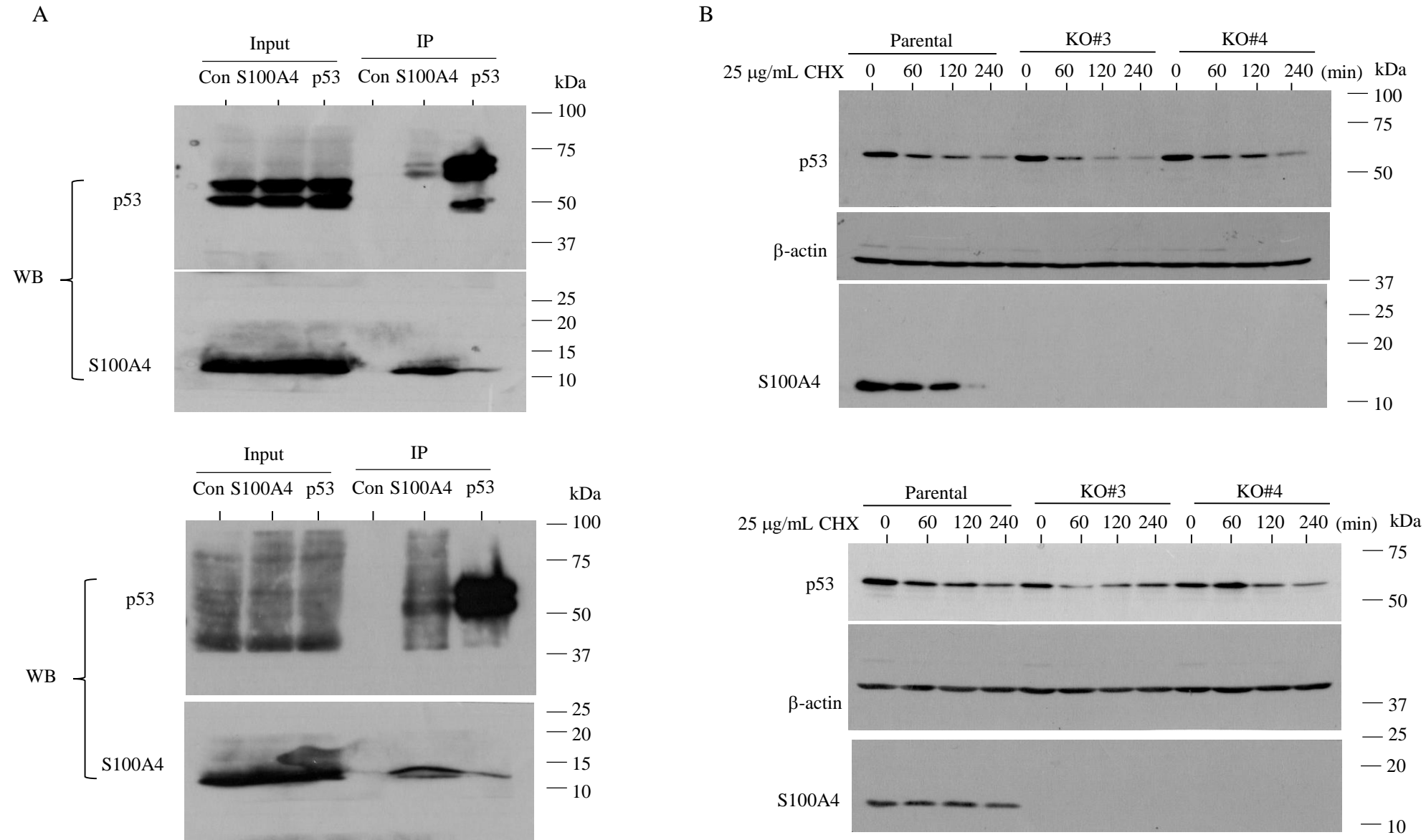


**Supplementary Figure S8.** Original images of western blot analysis for the indicated proteins in total lysates from HCT116-S100A4 KO and parental cells after 0.5 mg/mL ADR treatment. The reconstructed images of all blots with membrane edges visible are shown because some of the original full-length blots were cut prior to hybridization with antibodies (upper) and the replicate blots (lower).

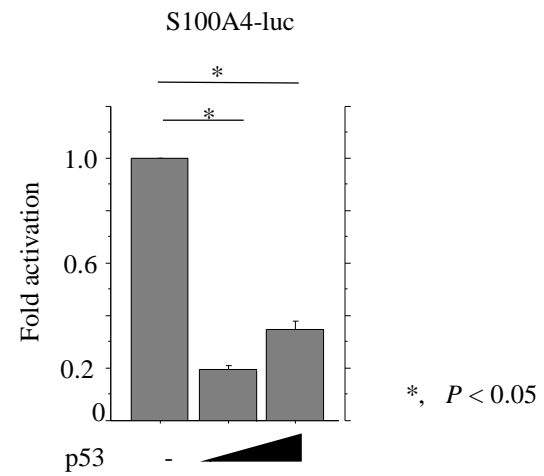




**Supplementary Figure S9.** Original images of western blot analysis for the indicated proteins in total lysates from HCT116-S100A4 KO and parental cells following re-stimulation of serum-starved (24 h) cells with 10% serum for the indicated times. The reconstructed images of all blots with membrane edges visible are shown because some of the original full-length blots were cut prior to hybridization with antibodies (upper) and the replicate blots (lower).



**Supplementary Figure S10.** Original images of western blot analysis for the indicated proteins in co-IP-western blot (A) and in total lysates from HCT116-S100A4 KO and parental cells treated with 25 mg/mL cycloheximide (CHX) at the indicated timepoints (B). The reconstructed images of all blots with membrane edges visible are shown because some of the original full-length blots were cut prior to hybridization with antibodies (upper) and the replicate blots (lower).



**Supplementary Figure S11. p53-dependent repression of the *S100A4* promoter.** HCT116 cells were transfected with *S100A4* promoter luciferase (luc), together with p53 using LipofectAMINE PLUS. Relative activity was determined based on arbitrary light units of luciferase activity normalized to pRL-TK activity. The activities of the reporter plus the effector relative to that of the reporter plus empty vector are shown as means  $\pm$  SDs. The experiments were performed in triplicate.